and the resultant 250 μL solution was incubated in the dark at 37°C for 15 h. In-solution digestion of the 26S proteasome sample was carried out as follows: 26S proteasome sample (50 μg) was diluted with ABC (aq., 50 mM) containing 10% v/v ACN to a final volume of approximately 190 μL. For reduction, 2.5 μL TCEP (10 mM) was added, and the solution mixture was kept at 37°C for 45 min. Subsequently, 2.5 μL IAM (50 mM) was added, and the solution mixture was alkylated in the dark at 24°C for 1 h. For digestion, trypsin (2 μg) was added to 5 μL ABC (50 mM), and 200 μL of the resulting solution was incubated in the dark at 37°C for 18 h. All reactions were performed in methylpentene polymer (TPX) microtubes (Hitech Inc. Tokyo, Japan) using an Eppendorf thermomixer R (Brinkmann, Westbury, NY, USA) for 1.5 mL microtubes; the resulting solution was interval-mixed (10 s) at 850 rpm. The digested 26S proteasome sample (50 μL) was diluted with 125 μL of 2% v/v ACN (aq.) containing 0.005% v/v TFA (aq.) after adjusting the pH to approximately 3 with 50 μL of 1% v/v TFA (aq.); the samples (25 μL) were then injected into the μLC-MS/MS system described in this paper.

2.3 Sample preparation of the digested human plasma protein mixture

The human blood plasma samples treated with heparin were obtained from Tokyo Medical University (Tokyo, Japan) and acquired from three, healthy, anonymous, male donors (samples: H-N, H-I, and H-S) and two male donors who were diagnosed with adenocarcinoma on the basis of clinical and laboratory criteria (stage: IIIA, samples: AC88 and AC94), after obtaining their informed consent. HSA and IgG in the human plasma samples (500 μL) was removed by affinity adsorption chromatography using Bio-Rad's Affi-Gel Blue Gel and protein A column (Bio-Rad Hercules, CA, USA), respectively (details not shown). The final concentration of the resulting HSA- and IgG-depleted human plasma (AID-HP) samples were 4.1 (H-N), 8.6 (H-I), 6.6 (H-S), 5.8 (AC88), and 7.2 mg/mL (AC94) in ABC (25 mM). Subsequently, 100 μL of the AID-HP sample was diluted with 400 μL ABC (25 mM) containing 32% v/v ACN. For reduction, 25 μL TCEP (50 mM) was added and the solution mixture was kept at 37°C for 45 min. Subsequently, 25 μL IAM (250 mM) was added and the solution mixture was alkylated in the dark at 24°C for 1 h. For digestion, trypsin (5 μg) was added and the resulting solution (555 μL) was incubated in the dark at 37°C for 16 h. All these reactions were carried out using the Eppendorf thermomixer R for 1.5 mL TPX microtubes, and the mixing was carried out at 850 rpm with periods and intervals of 10 s each. For the 1-D μLC-MS/MS analysis, the digested AID-HP samples (20 μL) were diluted with 20 μL of 1% v/v TFA (aq.) and 160 μL with 2% v/v ACN (aq.) containing 0.1% v/v TFA, in a TPX auto sampler tube; 20 μL of the resultant samples was injected into the system. In order to prepare individual mixture samples of the healthy and adenocarcinoma groups for 1-D and 2-D μLC-MS/MS analyses, 33.3 μL of each of the three AID-HP samples from the healthy group and 50 μL of each of the two AID-HP samples from the adenocarcinoma group were mixed with 100 μL of 1% v/v TFA (aq.), respectively; subsequently, 4 μL of the resulting sample solutions was used in these analyses.

2.4 1-D RP and 2-D SCX/RP μLC-NSI-MS/MS analyses

The 1-D and 2-D LC-MS/MS system with RP-μLC comprised a Paradigm MS4 dual solvent delivery system (Michrom BioResources, Auburn, CA, USA) for HPLC, an HTS PAL auto sampler with two 10-port injector valves (CTC Analytics, Zwingen, Switzerland), Finnigan LCQ Deca XP plus 3-D ion-trap, and Finnigan LTQ linear ITMS (Thermo Electron, San Jose, CA, USA) equipped with NSI sources (AMR Inc., Tokyo, Japan). Sample injection for the 1-D and 2-D μLC-MS/MS analyses as well as SCX separation for 2-D analysis were automatically carried out using the HTS PAL auto sample injection system with no change in the configurations. The SCX separation was performed on an SCX microtrap cartridge (12 μm, 300 Å, 8 × 1.0 mm i.d., Michrom) by stepwise elution on the first injector valve. The solvent system containing 2% v/v ACN was composed of 0.005% v/v TFA (aq.) and 1 M ammonium formate (aq.) adjusted to pH 2.8 with TFA, and the elution solvents (25, 50, 100, 150, 200, and 500 mM) were prepared by mixing these. The effluent from all the SCX fractions was flowed serially into a peptide CapTrap cartridge (2.0 × 0.5 mm i.d., Michrom), present on the second injector valve, for concentration and desalting. After desalting with 0.1% v/v TFA (aq.) containing 2% v/v ACN, the sample was loaded onto a capillary RP column, MAGIC C_{18} (3 μm, 200 Å, 50 × 0.2 mm i.d., Michrom), for 2-D separation. Digested samples for the 1-D RP analysis were also injected directly into a peptide CapTrap cartridge for concentration and desalting and then applied to RP separation. Solutions of 2% and 90% v/v ACN (aq.) were used as the mobile phases A and B, respectively, and both contained 0.1% v/v formic acid. The gradient conditions in the chromatographic run were as follows: B 5% (0 min) → 65% (20 min) for the digested samples of BSA and 26S proteasome, and B 5% (0 min) → 40% (70 min) → 95% (80 min) for plasma samples. Effluent solvent at 1.0–1.2 μL/min from the HPLC was introduced into the mass spectrometer by the NSI interface *via* an injector valve with a CapTrap cartridge and the RP column. The NSI needle (FortisTip, OmniSeparo-TJ, Hyogo, Japan), which was connected directly to the RP column outlet, was used as the NSI interface and the voltage was 1.8 kV, while the capillary was heated to 200°C [11]. No sheath or auxiliary gas was used. Further, the mass spectrometer was operated in a data-dependent acquisition mode in which MS acquisition with a mass range of m/z 450–2000 was automatically switched to MS/MS acquisition under the automated control of the Xcalibur software. The most intense ion of the full MS scan was selected as the parent ion and it was subjected to MS/MS scan with an isolation width of m/z 2.0; the activation amplitude parameter

was set at 30%. For the human plasma samples, the full MS scan was acquired followed by two successive MS/MS scans of the two most intense precursor ions detected in the full MS scan. The trapping time was 100 ms under the auto gain control mode. Data was acquired using the dynamic mass-exclusion windows that had an exclusion of 3.0-min duration and exclusion mass widths of −0.5 and +1.5 Da.

2.5 Database searches

All MS/MS data were investigated using the Mascot search engine (Matrix Science, London, UK) [12] against the Swiss-Prot database. The data acquired for BSA digests were investigated against other mammalian subsets of the sequences. The MS/MS data of the human 26S proteasome and plasma samples were investigated against the *Homo sapien* subsets of the sequences. The database searches allowed for fixed modification on the cysteine residue (carbamidomethylation, +57 Da), variable modification on the methionine residue (oxidation, +16 Da), peptide mass tolerance at ±2.0 Da, and fragment mass tolerance at ±0.8 Da.

3 Results and discussion

3.1 Evaluation of the μLC-MS/MS analysis using the linear 2-D ITMS instrument

We developed the μLC-MS/MS system with RP separation (1-D RP), which corresponds to the second dimension separation for the on-line and off-line 2-D μLC-MS/MS system [9, 10]. This system comprises a microflow LC system with a variable splitter, a versatile auto-sampler equipped with an injector valve, and a LCQ 3-D (ITMS) with an NSI stage. A flow rate of 1.0–1.2 μL/min *via* the injector valve and the RP column (0.2 mm i.d.) has been adopted as a convenient and efficient condition for routine proteome analysis with high sensitivity and reproducibility. The detection limit for identification of proteins in protein digests was approximately a few fmol. In order to evaluate the sensitivity of the new linear 2-D ITMS instrument (LTQ) for protein identification, we connected our RP μLC system to the LTQ instead of the conventional 3-D ITMS (LCQ) instrument. BSA digests (5–500 fmol) were applied to μLC-MS/MS analysis using the LTQ and LCQ instruments under identical conditions except those used for the mass spectrometer. The base-peak chromatogram for BSA digests (500 fmol) is shown in Fig. 1a. A comparison of the coverage, in terms of protein identification, between the LCQ and LTQ instruments revealed that 25% coverage of the BSA sequence was acquired from 5 fmol of the digests using the LTQ instrument, as shown in Fig. 2. Since the same coverage was obtained from 50 fmol of the digests using the LCQ instrument, the results indicated that the protein identification improved markedly as the sensitivity increased 10-fold using the LTQ instrument.

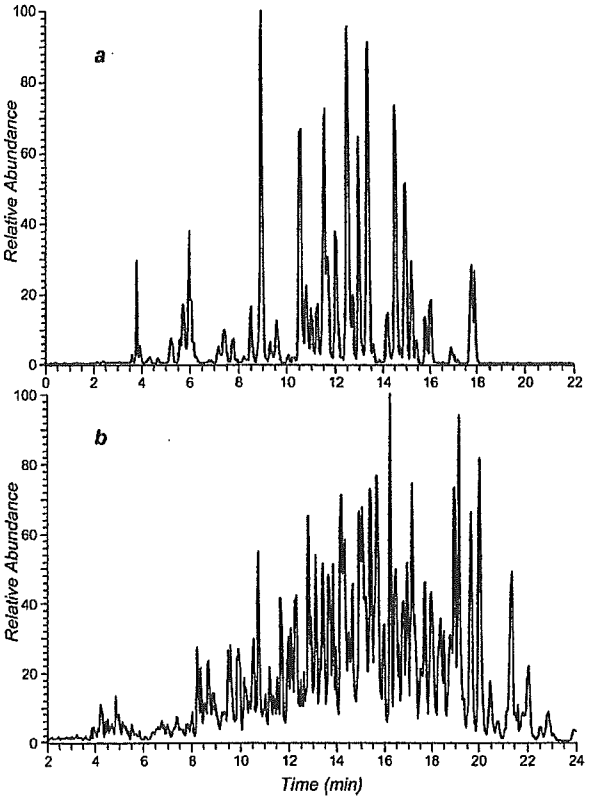

Figure 1. Base-peak chromatograms of the digested BSA (a) and 26S proteasome (b) using 1-D RP μLC-MS/MS analysis.

A dramatic improvement is achieved in the LTQ instrument in terms of the scan speed, which is higher than that of conventional 3-D ITMS instruments. Figures 3a and 3b show the expanded mass chromatograms with stick plotting at *m/z* values 710.0–711.5 obtained by μLC-MS/MS analysis of BSA digests using the LTQ and LCQ instruments, respectively. A stick in the peak represents a single full MS or MS/MS scan. The range denoted by the arrow in Fig. 3 shows that 62 events that carried out the acquisition of a full MS and an MS/MS spectra were achieved by the LTQ instrument in comparison with 12 events acquired by the LCQ instrument in 30 s. When conventional LCQ instruments are used, we usually apply three and two microscans for full MS (50 ms trapping time) and MS/MS (200 ms) accumulations, respectively, in order to obtain a better quality spectrum from a single scan. On the other hand, both spectra for peptide sequencing in protein identification were effectively acquired by one microscan of both full MS (50 ms) and MS/MS (100 ms) accumulations by LTQ instrument. As a result, using the LTQ instrument, it is possible to obtain an approximately five-fold higher number of MS/MS spectra in the same analytical run time.

In general, it is necessary to acquire a greater number of MS/MS spectra for the identification of a greater number of proteins using peptide sequencing. In studies where LC-MS/

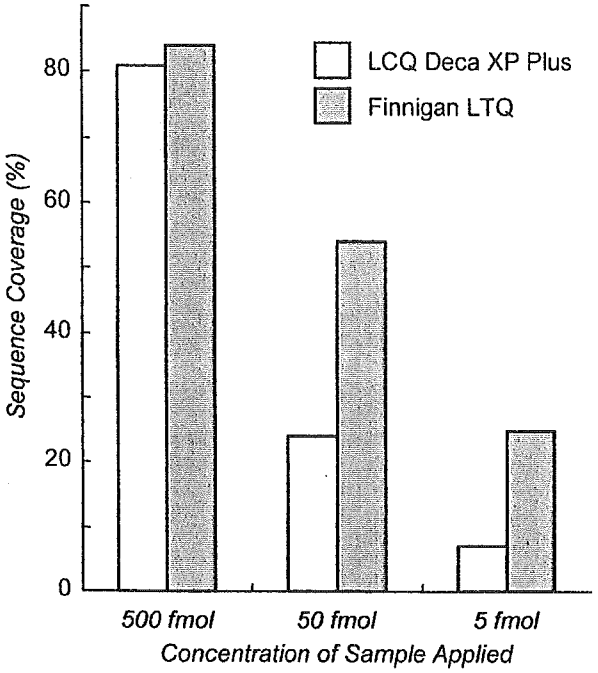

Figure 2. Comparison of sequence coverage of BSA digests (5–500 fmol) by μLC-MS/MS analysis using LCQ Deca XP plus 3-D ion-trap and Finnigan LTQ linear ion-trap MS instruments.

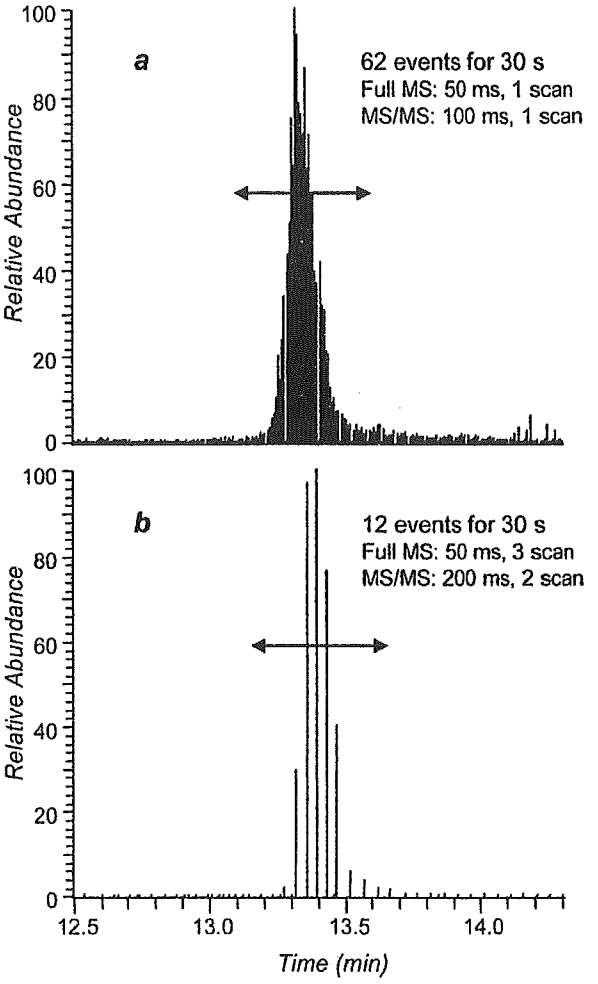

Figure 3. Mass chromatograms at *m/z* 710.0-711.5 by μLC-MS/MS analysis of BSA digests using Finnigan LTQ (a) and LCQ Deca XP plus (b) instruments. A stick in the peak is a single full MS and MS/MS scan of the mass spectrometer, and 62 and 12 events (acquisition of a full MS and a MS/MS in one event) were carried out by the LTQ and LCQ instruments, respectively.

MS was used for comprehensive proteome analysis, several researchers investigated various methods to data-dependently amass MS/MS spectra for a single analysis. These methods include employing a longer analytical time, triple and more MS/MS acquisition against a single full MS spectrum, multiple analyses of the same sample using common conditions or fractionated mass range, etc. While obtaining the MS/MS spectra, the scan speed is a mechanical limitation and a data-dependent scan misses many of the peptide sequences for low abundance peaks that are behind large peaks. Therefore, it is necessary to choose the applications of these techniques for comprehensive proteome analysis of highly complex protein mixtures such as human plasma and whole cell lysates. The drawbacks of clinical proteomics for a large number of human samples are the inability to conduct multiple analyses of the same sample and the longer running time required by the comprehensive LC-MS/MS analysis. Consequently, the performance of the LTQ instrument with a higher scan speed is better than that of the conventional 3-D ITMS instrument, because it enables more informative high-throughput LC-MS/MS analysis for highly complex clinical samples. Therefore, to verify the applicability of LTQ instruments, the human 26S proteasome, which is a highly complex protein mixture consisting of 31 components, was subjected to analysis. As shown in Fig. 1b, equivalent amounts of the digested 26S proteasome sample were analyzed using the LCQ and LTQ instruments under identical μLC conditions. The data-dependent MS/MS acquisition, in which the full MS acquisition is followed by a single MS/MS scan of the most intense precursor ion obtained from the full MS scan, was applied with three microscan full MS (50 ms trapping time) and two microscan MS/MS (200 ms) accumulations for the LCQ, and one microscan of both full MS (50 ms) and MS/MS (100 ms) accumulations for the LTQ instruments. During the 20 min analysis, approximately 450 and 2200 MS/MS spectra were obtained from the 1-D RP μLC-MS/MS analyses using the LCQ and LTQ instruments, respectively. These data were evaluated using a Mascot database search against the Swiss-Prot database, and the search results obtained for the peptide MS/MS assignment were filtered based on the criterion defined as a Mascot peptide score more than 20 and ranked first, described in detail below. Table 1 (see also Supplemen-

Table 1. Protein identification results of human 26S proteasome.

Protein	LCQ Deca XP Plus			Finnigan LTQ		
	Score	Coverage	Peptide	Score	Coverage	Peptide
26S protease regulatory subunits						
PRS4	221	13	3	851	41	16
PRS6	142	9	3	757	48	16
PRS7	348	15	5	1346	55	23
PRS8	299	16	4	1304	58	20
PRSA	377	21	7	1093	53	19
PRSX	154	7	2	715	36	12
Proteasome subunit alpha types						
PSA1	494	36	8	658	48	11
PSA2	261	18	4	569	56	9
PSA3	145	13	3	584	43	11
PSA4	115	9	2	459	33	7
PSA5	158	17	3	483	47	8
PSA6	559	38	8	700	48	11
PSA7	423	35	7	772	57	12
Proteasome subunit beta types						
PSB1	275	34	5	596	53	10
PSB2	256	24	4	456	43	8
PSB3	235	24	3	379	35	5
PSB4	117	9	2	511	48	8
PSB5	528	42	7	670	58	10
PSB6	200	13	3	271	24	5
PSB7	232	14	4	381	33	7
PSB8	ND	ND	ND	180	18	4
26S proteasome non-ATPase regulatory subunits						
PSD1	227	6	3	1636	38	27
PSD2	380	10	6	1386	34	26
PSD3	690	24	10	1445	50	25
PSD4	74	5	1	358	22	6
PSD6	206	12	3	1001	46	18
PSD7	250	15	3	487	42	10
PSD8	ND	ND	ND	228	19	5
PSDB	571	22	8	1445	59	23
PSDC	359	15	5	1147	37	20
PSDD	183	10	4	966	52	17
		Total	130		Total	409

The protein identification data of 31 components consisted of human 26S proteasome including the number of the peptide fragments assigned (Peptide) and the sequence coverage according to these peptides (Coverage). The protein score is calculated by the addition of these peptide scores (Score) in comparison to 1-D μLC-MS/MS analysis using conventional 3-D ion-trap MS (LCQ Deca XP Plus) and new linear ion-trap MS instruments (Finnigan LTQ). ND, not detected.

tary Table A) shows protein identification results including the number of peptide fragments assigned, sequence coverage with these peptides, and the protein score calculated by addition of these peptide scores with respect to the 31 components of the 26S proteasome. In the case of the LTQ instrument, 409 peptide fragments were assigned as components of the 26S proteasome, and this number was approximately three-fold higher than that obtained when the LCQ instrument was used (130 peptide fragments). The individual components of the 26S proteasome were identified by 13.2 and 4.5 peptide fragments, 43.0% and 18.1% sequence coverage, and 821.9 and 292.4 protein scores on an average, using the LTQ and LCQ instruments, respectively. Twenty-nine proteins in 31 components were identified even by the LCQ instruments using our RP μLC system with high-resolution power, as shown in Fig. 1b. However, the peptide fragments of the remaining two components were not observed from the filtered database search results. A number

of peptide fragments belonging to the 26S proteasome (>700 peptides and >60% coverage on an average) were detected by an on-line 2-D SCX/RP μLC-MS/MS experiment with the same amount of digests using the LCQ instrument [10]. These results may simply indicate the difference in the scan speed for the limited, short analytical time between the LCQ and LTQ instruments and not a difference in the sensitivity. Accordingly, LC-MS/MS analysis using LTQ has a three-fold higher efficiency in identification in comparison with a conventional LCQ. This indicates that the LTQ has a superior protein identification capability. Thus, the introduction of LTQ into our μLC-MS/MS system resulted in a highly improved performance, in terms of both sensitivity and protein identification efficiency, for highly complex mixtures.

3.2 Human plasma proteome analysis

The usefulness and applicability of our automated protein profiling system coupled with LTQ for clinical proteomics have been examined by analyzing human plasma samples. In the course of clinical plasma proteome studies, we investigated two types of human plasma – one from healthy donors and the other from donors with lung adenocarcinoma. All plasma samples obtained from the three healthy (H-N, H-I, and H-S) and two adenocarcinoma (AC88 and AC94) cases were digested in a solution with trypsin after removing their HSA and IgG contents. The resultant peptide mixtures were diluted for the μLC-MS/MS analysis. Further, equivalent mixture samples from the three healthy donors (H-NIS; H-N:H-I:H-S, 1:1:1 in volume) and the two adenocarcinoma donors (AC8894; AC88:AC94, 1:1 in volume) were also prepared as average samples for each case. The individual and mixture samples (total seven samples) were analyzed by 1-D RP μLC-MS/MS analysis under analytical conditions for 90 min. The LTQ MS data was acquired by the double MS/MS method, in which the full MS acquisition is followed by two MS/MS scans of the two most intense precursor ions from the full MS scan. This is done to improve the protein identification results by the database search. Additionally, our established on-line 2-D SCX/RP μLC-MS/MS system using LTQ instead of the conventional LCQ instrument was also used to analyze the mixture samples (H-NIS and AC8894) along with an additional 1-D RP analysis. In the 2-D μLC-MS/MS analysis, six SCX separation runs were automatically carried out and analyzed by the RP μLC-MS/MS analysis under the same analytical conditions as described earlier. The total operation time for both 1-D and 2-D μLC-MS/MS analyses of a sample was within 11 h [10]. Figure 4 shows the base-peak chromatograms from 1-D (g) and 2-D

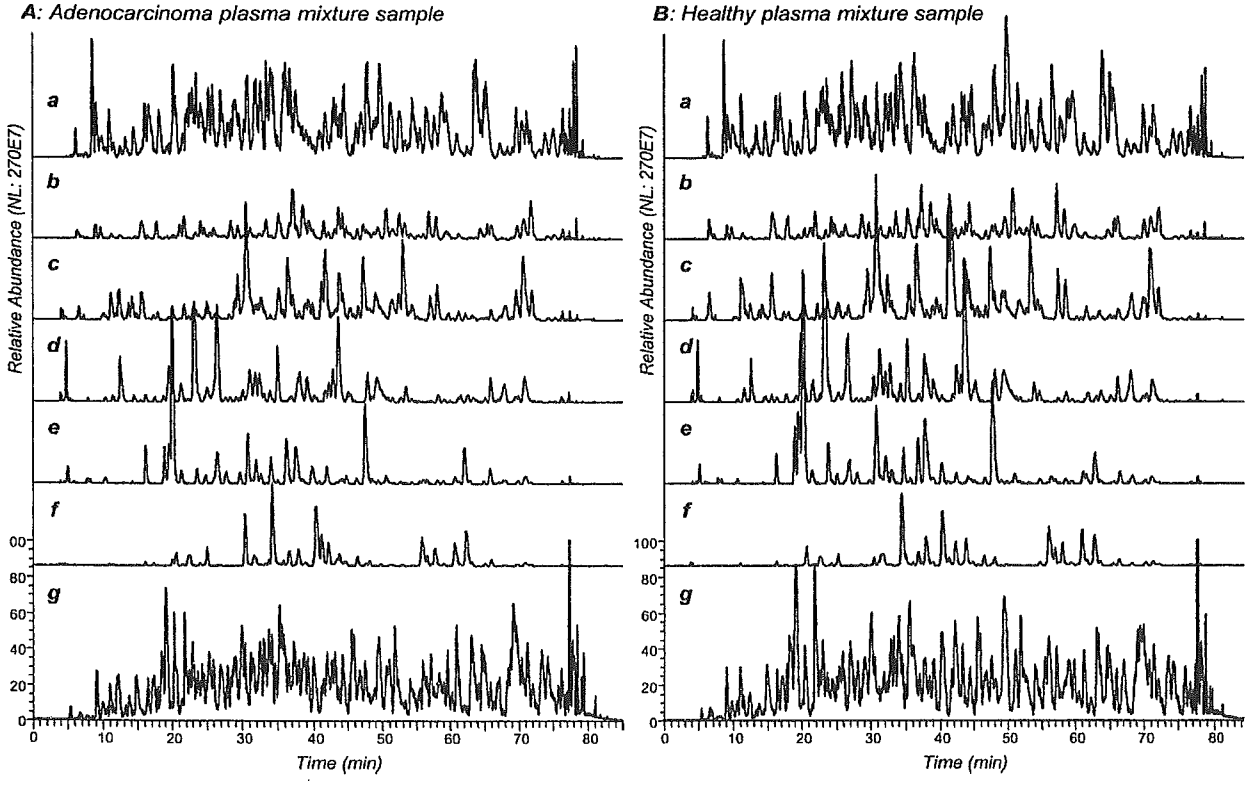

Figure 4. Base-peak chromatograms of the digested human plasma samples using 2-D SCX/RP (a–f) and 1-D RP μLC-MS/MS analyses (g). A, mixture of plasma digests of the healthy group; B, mixture of plasma digests of the adenocarcinoma group; a, 25 mM; b, 50 mM; c,100 mM; d, 150 mM; e, 200 mM; f, 500 mM salt concentration SCX fractions for 2-D μLC-MS/MS analysis.

μLC-MS/MS analyses (a–f) of approximately 2 μg AID-HP tryptic digests corresponding to 0.4 μL original blood plasma sample. The 1-D RP μLC-MS/MS analysis provided approximately 10 000 MS/MS spectra for each sample, and the resultant data were evaluated using a Mascot database search against *H. sapien* subsets of the sequences in the Swiss-Prot database.

In order to achieve statistical confidence levels in identification of proteins from highly complex mixture samples, we investigated the thresholds as filters to extract data for the Mascot peptide score. We used the datasets, obtained from the 1-D μLC-MS/MS analysis with LTQ, of the digested 26S proteasome sample within our search tolerances. Since it is possible to identify several proteins from a single MS/MS spectrum based on the hit sequence varieties, the most significant peptide sequence that was ranked first (marked with bold red in the Mascot search results), which had the highest score among the hit varieties, was extracted from the entire datasets to prevent erroneous identifications and redundancy. The resulting peptide assignments were sorted according to their Mascot peptide score and intergraded into protein identification. Figure 5 (see also Supplementary Table A) shows the relationship between the peptide score ranges and either the number of peptide fragments assigned as 26S proteasome or other proteins identified erroneously. Although peptides with a score less than 50 were assigned to both the 26S proteasome and to the other proteins, all peptide fragments with a score of more than 50 were confidently identified as belonging to the 26S proteasome. For thresholds of peptide scores higher than 20, 30, and 40, the statistical identification confidence levels of the Mascot database search results were 70%, 90%, and 97%, respectively. Accordingly, we tentatively set peptide scores more than 30 and ranked first as the criterion for a broad protein identification index in order to integrate the datasets of the μLC-MS/MS analysis of plasma samples. Furthermore, to extract plasma proteins with a higher confidence level, we finally tried to apply the Swiss-Prot dataset (667 proteins) in a non-redundant list of 1175 distinct proteins that Anderson *et al.* have recently developed by combining four separate sources of human plasma proteome [3, 13–16].

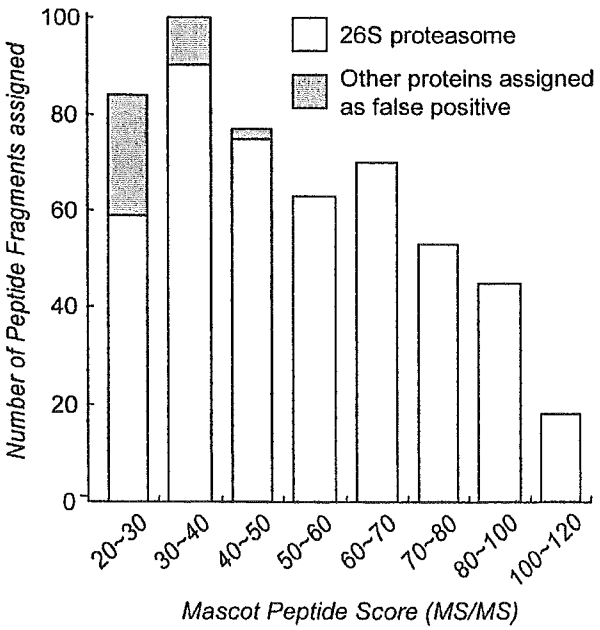

Figure 5. Mascot database search results of 1-D μLC-MS/MS analysis of the digested 26S proteasome. See also Supplementary Table A.

The Mascot database search results on plasma proteome analysis yielded data extracted under the thresholds of peptide scores higher than 30 and ranked first; an average of 108 proteins were detected from each 1-D μLC-MS/MS analysis. From the 2-D μLC-MS/MS analysis of the mixture sample of two groups, an average of 249 proteins was assigned as plasma proteome candidates. (Supplementary Table B). Additionally, entire datasets of these Mascot search results were integrated and processed with the data extraction. The results indicated that a total of 506 different proteins were listed, and 180 proteins were detected as common proteins from both groups (Fig. 6, in parentheses). Furthermore, plasma proteins with a high confidence level were extracted from these datasets using the Swiss-Prot dataset of the 667 plasma proteins reported. Figure 6 shows the diagrammatic representation of proteins found in the two groups comprising healthy individuals and adenocarcinoma patients, and the numbers are concordant with the proteins annotated as plasma proteins in 667 Swiss-Prot datasets. The results indicated that 84 and 85 proteins were extracted from the healthy and adenocarcinoma groups, respectively, and 69 proteins were common. In addition, 16 proteins were

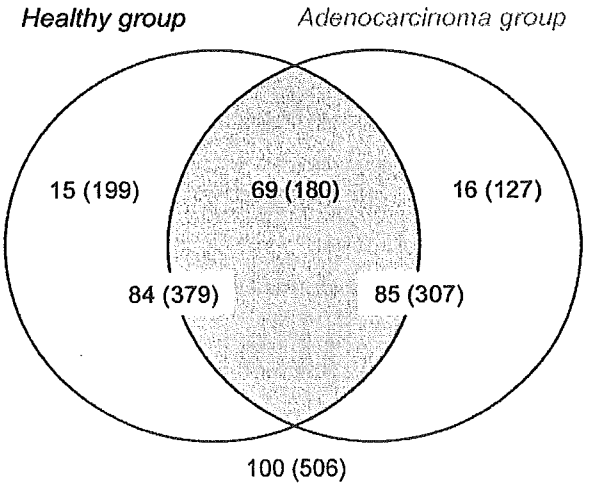

Figure 6. Diagrammatic representation of the proteins detected in the groups of healthy individuals and adenocarcinoma patients by 1-D and 2-D μLC-MS/MS analyses of their plasma samples. Numbers that belong to the peptide score thresholds higher than 30 served as the criteria for protein extraction (expressed in parentheses), and the numbers are concordant with the plasma proteins reported in the 667 Swiss-Prot datasets.

Table 2. Selected specific protein list of the healthy and lung adenocarcinoma groups in human blood plasma.

Accession No.	Protein name	Adenocarcinoma plasma samples					Healthy plasma samples					
		2-D analysis	1-D μLC-MS/MS analysis				2-D analysis	1-D μLC-MS/MS analysis				
		AC8894	AC88	AC94	AC8894-1	AC8894-2	H-NIS	H-N	H-I	H-S	H-NIS-1	H-NIS-2
P02649	Apolipoprotein E	A	C	A	A	A			C			
Q14624	Inter-alpha-trypsin inhibitor heavy chain H4	A	C	B	C		C		C	C	C	C
P04196	Histidine-rich glycoprotein	A										
P00748	Coagulation factor XII	B										
P00488	Coagulation factor XIII A chain	B					C					
P02570	Actin, cytoplasmic 1	C					A	A	C		C	
P27169	Serum paraoxonase/arylesterase 1						A					
P29312	14-3-3 protein zeta/delta								A			
P54108	Cysteine-rich secretory protein-3	C					B					
Q14791	Apolipoprotein L1						B					
P02751	Fibronectin						B					
P06396	Gelsolin, plasma						B					

Two adenocarcinoma plasma samples (AC88 and AC94) and three healthy plasma samples (H-N, H-I, and H-S) were analyzed by 1-D μLC-MS/MS analysis. The mixture samples separated into both groups (AC8894 and H-NIS) were analyzed twice by 1-D and once by 2-D μLC-MS/MS analysis (2-D analysis). A–C indicated the presence of peptide fragment(s) assigned to the listed protein. A, mascot peptide score higher than 50; B, score 40 to 50; C, score 20 to 40. See also Supplementary Table B.

detected as specific significant proteins of the adenocarcinoma group, and 15 proteins were not detected in the adenocarcinoma group. Table 2 (see also Supplementary Table B) shows a list of the specific proteins assigned by peptide fragment(s) with scores higher than 40. These specific proteins detected from only one group might be candidate biomarkers of lung adenocarcinoma in human blood plasma. However, further statistical verification of our results through data accumulation of more disease plasma samples and the investigation concerning the reproducibility of protein identifications for each sample are necessary. Additionally, validation of these protein identifications by several biochemical approaches would be required. In the present study, we could indicate that several significant protein candidates in the plasma proteome are possibly associated with the pathological differences in lung adenocarcinoma. Functions of specific proteins and their correlations with adenocarcinoma along with the other proteins are not listed in this paper and will be reported elsewhere. These experimental achievements suggest that our automated 1-D and 2-D μLC-MS/MS protein profiling systems, in which the LTQ was incorporated, are powerful in identifying low-abundance proteins of great clinical importance, because these molecules directly report the occurrence and progress of various diseases.

4 Concluding remarks

In the course of the Human Plasma Organization Plasma Proteome Project, several research groups have prepared contrast reference specimens of human plasma using various technology platforms [17]. It is extremely important to catalog the plasma proteome as a protein database for clinical plasma proteomics. Applied technology platforms are very powerful, particularly for comprehensive broad protein identification of highly complex samples such as blood plasma. However, it seems difficult to stably and reproducibly apply these to routine clinical investigations that require a large number of proteome analysis runs for a large number of human samples. We have recently established a fully automated, high-throughput 2-D SCX/RP μLC-MS/MS protein profiling system, which can perform large-scale analysis in clinical proteomics [10]. In this study, the LTQ, which is superior to a conventional 3-D ITMS instrument in sensitivity and scan speed, was utilized in our high-throughput system, and it was evaluated by analyzing BSA and human 26S proteasome. Furthermore, the system was applied to plasma proteome analysis in a few cases of both healthy individuals and lung adenocarcinoma patients. The results confirmed that a 10-fold increase in terms of sensitivity was achieved in our system using the LTQ instrument for protein

identification. Further, in comparison with the conventional 3-D ITMS instrument, a three-fold higher number of peptide fragments was identified as belonging to the 26S proteasome, indicating significant improvement in resolution for the analytical time point. Additionally, approximately 250 and 100 different proteins were detected, based on the investigation criterion for a 90% confidence level of protein identification, from only 0.4 μL human plasma using 2-D and 1-D μLC-MS/MS analyses, respectively. The entire operation was automatically carried out within 11 h for both single 1-D and 2-D μLC-MS/MS analyses. From the protein identification datasets of both healthy and adenocarcinoma plasma samples, several disease-specific proteins were found in the human plasma based on the plasma proteome database reported earlier. Consequently, it was demonstrated that our μLC-MS/MS protein profiling system is feasible for large-scale analyses such as clinical plasma proteomics studies. Although plasma proteome analysis for clinical application still remains a great challenge due to the wide dynamic range of protein abundance, we shall continue further technological development of the large-scale proteome analysis based on the high-throughput μLC-MS/MS system reported in this paper. Such high-throughput and large-scale analysis of human plasma would lead to the discovery of new disease-associated protein markers with high sensitivity and high specificity in early disease detection and diagnosis, and this would revolutionize current therapeutics.

The authors gratefully acknowledge the technical assistance of Ms. Hisae Anyoji and Noriko Araki of Medical Proteoscope, Co. Inc., and medical doctors of the Department of Surgery, Tokyo Medical University, as well as the encouragement and support of AMR Inc., Tokyo, Japan. We are also deeply indebted to Drs. Hiroshi Matsumoto and Masayuki Kubota of Thermo Electron Co., Kanagawa, Japan for their assistance.

5 References

[1] Liotta, L. A., Ferrari, M., Petricoin, E., *Nature* 2003, *425*, 905.

[2] Anderson, N. L., Anderson, N. G., *Mol. Cell. Proteomics* 2002, *1*, 845–867.

[3] Anderson, N. L., Polanski, M., Pieper, R., Gatlin, T. *et al.*, *Mol. Cell. Proteomics* 2004, *3*, 311–326.

[4] Washburn, M. P., Wolters, D., Yates, J. R. III, *Nat. Biotechnol.* 2001, *19*, 242–247.

[5] Wolters, D. A., Washburn, M. P., Yates, J. R., III, *Anal. Chem.* 2001, *73*, 5683–5690.

[6] Shen, Y., Jacobs, J. M., Camp, D. G., II, Fang, R. *et al.*, *Anal. Chem.* 2004, *76*, 1134–1144.

[7] Kawakami, T., Nagata, T., Muraguchi, A., Nishimura, T., *Electrophoresis* 2000, *21*, 1846–1852.

[8] Kawakami, T., Nagata, T., Muraguchi, A., Nishimura, T., *J. Chromatogr. B* 2003, *87*, 223–229.

[9] Fujii, K., Nakano, T., Kawamura, T., Usui, F. *et al.*, *J. Proteome Res.* 2004, *3*, 712–718.

[10] Fujii, K., Nakano, T., Hike, H., Usui, F. *et al.*, *J. Chromatogr. A* 2004, *1057*, 107–113.

[11] Tojo, H., *J. Chromatogr. A* 2004, *1056*, 223–228.

[12] http://www.matrixscience.com

[13] Pieper, R., Su, Q., Gatlin, C. L., Huang, S. T. *et al.*, *Proteomics* 2003, *3*, 422–432.

[14] Adkins, J. N., Varnum, S. M., Auberry, K. J., Moore, R. J. *et al.*, *Mol. Cell. Proteomics* 2002, *1*, 947–955.

[15] Tirumalai, R. S., Chan, K. C., Prieto, D. A., Issaq, H. J. *et al.*, *Mol. Cell. Proteomics* 2003, *2*, 1096–1103.

[16] Pieper, R., Gatlin, C. L., Makusky, A. J., Russo, P. S. *et al.*, *Proteomics* 2003, *3*, 1345–1364.

[17] Omenn, G. S., *Proteomics* 2004, *4*, 1235–1240.

Int J Clin Oncol (2005) 10:157–164
DOI 10.1007/s10147-005-0493-x

FROM THE ASCO-JSCO JOINT SYMPOSIUM

Harubumi Kato · Masahiro Tsuboi · Yasufumi Kato
Norihiko Ikeda · Tetsuya Okunaka · Chikuma Hamada

Postoperative adjuvant therapy for completely resected early-stage non-small cell lung cancer

Received: March 30, 2005

Abstract Consensus on adjuvant therapy for completely resected non-small cell lung cancer until 2002 was as follows. (1) There was no significant impact of postoperative adjuvant chemotherapy based on meta-analysis and previous clinical trials. (2) Confirmatory studies are necessary in large-scale prospective clinical trials. However, recent mega trials have introduced epoch-making changes for postoperative adjuvant chemotherapy in clinical practice since ASCO 2003. The effectiveness of UFT in N0 patients was confirmed. Patients with completely resected stage I non-small cell lung cancer, especially T2N0 adenocarcinoma, will benefit from adjuvant chemotherapy with UFT. The results of the International Adjuvant Lung Trial (IALT) have confirmed the meta-analysis in 1995. Also, both the JBR10 and Cancer and Leukemia Group B (CALGB) 9633 studies have also confirmed positive IALT results of the benefit for postoperative platinum-based chemotherapy in completely resected non-small cell lung cancer. Adjuvant chemotherapy for pathological stage IB to II, completely resected non-small cell lung cancer is standard care based on clinical trials. UFT showed the strongest evidence for IB in Japan. Platinum doublet chemotherapy with third-generation anticancer agents is also recommended. Adjuvant chemotherapy should be offered as standard care to patients after completely resected early stage non-small cell lung cancer. However, there is no evidence of the feasibility and efficacy for adjuvant chemotherapy with the platinum-based regimen in Japan. Careful management should be necessary in such treatment.

Key words Adjuvant therapy · Chemotherapy · Surgery · Non-small cell lung cancer · Early-stage lung cancer

Introduction

The 5-year survival rate after surgical treatment in the United States and Japan in each stage of non-small cell lung cancer is shown in Table 1.[1,2] Although these surgical outcomes reveal the slight difference among two groups, we are not satisfied with the results, particularly in stage IB and II, which are so-called early stage. Surgery is still the best therapeutic modality for the potential cure of the patient with non-small cell lung cancer, especially in stage I. However, in the patient with pathological stage IB, the 5-year survival rate is only about 60%. The recurrence pattern is frequently due to distant metastasis.[3] Therefore, perioperative adjuvant therapy is required for improvement of survival after surgical resection.

Meta-analysis of the randomized trials of adjuvant therapy of non-small cell lung cancer in 1995 suggested the survival benefit of cisplatin-based chemotherapy after surgery.[4] However, there are no statistical differences between postoperative adjuvant group and surgery alone,[4] and this includes a number of small trials and trials with the following disability criteria and chemotherapy regimens.

Consensus on adjuvant therapy for completely resected non-small cell lung cancer up to 2002 was as follows: (1) there was no significant impact of postoperative adjuvant chemotherapy based on meta-analysis and previous clinical trials. (2) Confirmatory studies are necessary in large-scale prospective clinical trials.[5–10] However, recent mega trials have introduced epoch-making changes for postoperative adjuvant chemotherapy in clinical practice since ASCO 2003.[11–19]

H. Kato · M. Tsuboi (✉) · Y. Kato
Department of Surgery, Tokyo Medical University, 6-7-1 Nishi-shinjuku, Shinjuku-ku, Tokyo 160-0023, Japan
Tel. +81-3-3342-6111, Fax +81-3-3349-0326
e-mail: mtsuboi@za2.so-net.ne.jp/Tsuboi0120@aol.com

N. Ikeda · T. Okunaka
Department of Thoracic Surgery, International University of Health and Welfare, Tokyo, Japan

C. Hamada
Faculty of Engineering, Tokyo University of Science, Tokyo, Japan

The ASCO-JSCO Joint Symposium was held in Kyoto, Japan, on October 29, 2004.

Table 1. The surgical outcome for resected non-small cell lung cancer: 5-year survival rate (%)

Stage	Clinical staging		Pathological staging	
	Mountain	Japan	Mountain	Japan
IA	61	72.1	67	79.5
IB	38	49.9	57	60.1
IIA	34	48.7	55	59.9
IIB	24	40.6	39	42.2
IIIA	22	35.8	38	29.8
IIIB	9	28.0	3–7	19.3
IV	13	20.9	1	20.0

The new paradigm shift for the adjuvant treatment after surgery is demonstrated here by the Japanese and international trials that have been reported since 2003.

Japanese trials

A large-scale randomized phase III study of postoperative adjuvant chemotherapy with UFT for p-stage I adenocarcinoma: the JLCRG (Japan Lung Cancer Research Group) trial (presented in ASCO 2003[13])

The oral antimetabolite UFT is composed of tegafur and uracil mixed at the ratio of 1:4. This drug has been developed by Taiho Pharmaceutical Corporation, Tokyo, Japan. UFT produced higher levels of 5-FU without the toxic level of 5-FU.

Concerning adjuvant treatment using UFT, the West Japan Study Group for Lung Cancer Surgery reported that postoperative adjuvant treatment with UFT in patients with completely resected stage I–III disease prolonged survival significantly longer than observation alone. The 5-year and 10-year survival rates were 64% and 48% in the UFT group, and 49% and 32% in the control group, respectively (P = 0.02).[11] In a subgroup analysis, no statistically significant difference in the overall survival of patients with squamous cell carcinoma between the two groups was observed (P = 0.24). In contrast, the patients with adenocarcinoma in the UFT group had a significantly better survival than those in the control group (P = 0.009).[12] In addition, most patients with adenocarcinoma had stage I disease. This trial demonstrated that UFT was useful in postoperative adjuvant chemotherapy against the earlier stage of non-small cell lung cancer. However, this study involved issues with respect to study design, because enrolled subjects varied from stage I to III, with a broad range of outcome. Those results prompted us to conduct a prospective randomized trial of UFT as a postoperative adjuvant treatment for patients whose stage I adenocarcinoma was completely resected. In the confirmatory study conducted by the Japan Lung Cancer Research Group (JLCRG), patients with completely resected pathological stage I adenocarcinoma of the lung were randomized with stratification according to their pathological T status (T1 versus T2), gender, and age, which were separated between less than 65 years old and 65 years old or over, to either receive the oral administration of UFT (tegafur 250 mg/m^2/day) for 2 years or no treatment. The patients with limited resection, such as wedge resection, were excluded. A follow-up examination was performed every 3 months for the first 2 years after the patient's operation and every 6 months thereafter. The primary endpoint was overall survival.

From January 1994, through March 1997, 999 patients were entered into the study. Twenty patients withdrew their informed consent or were found to be ineligible before the start of treatment. The number of eligible randomized patients was 491 in the UFT group and 488 in the nontreatment control group. Main patient characteristics were as follows: men, 48.7%; more than 65 years old, 43.9%; pathological T1, 73.1%. There were no significant differences in the baseline characteristics of the patients. The median duration of follow-up for all 979 patients was 73 months, with range 61–94 months.

Few severe adverse reactions were associated with UFT administration. There was no grade 4 adverse reaction. In total, 10 (2%) of 482 patients developed a grade 3 adverse reaction. The percentage of compliance for UFT administration was calculated based on the number of patients who actually took UFT and the number of patients without recurrence, second cancer, or death who were expected to take UFT. The percentage of compliance was 80% [95% confidence interval (CI), 77%–84%) at 6 months, 74% (95% CI, 70%–78%) at 12 months, 69% (95% CI, 65%–73%) at 18 months, and 61% (95% CI, 77%–84%) at 24 months. The main reasons for discontinuation of UFT administration were as follows: an adverse reaction in 123 patients, patient refusal in 52, and the doctor's judgment in 34.

Overall survival between the two groups showed a statistically significant difference in favor of the UFT group based on a Kaplan–Meier analysis (P = 0.04). The 5-year survival rate (5YS) was 87.9% in the UFT group and 85.4% in the control group, respectively. Treatment failure was documented in 22.6% of the patients in the UFT group and 26.4% in the control group, respectively. The most frequent failure pattern was distant metastasis in both groups. The 5-year cancer-free survival rate was 82.8% in the UFT group and 80.4% in the control group. There is no significant difference between the two groups at P = 0.25.

Concerning subset analysis of pathological T factors, although there was no statistical difference in the T1 population, in the T2 subset, the 5-year survival rate was 84.9% in the UFT group and 73.5% in the control group. The hazard ratio was 0.0842 in the UFT group with a clear statistical difference (P = 0.0051). Concerning interaction in relation to treatment effect, treatment with UFT tended to improve the survival rate among the patients with tumors that were 2–3 cm in diameter and provided 30% survival benefit for patients with tumor that was more than 3 cm in diameter. These findings indicated that the effect of UFT might be related to certain biological factors.

In conclusion, oral demonstration with UFT in the postoperative adjuvant setting yielded a significant improvement in survival in patients with pathological stage I adenocarcinoma of the lung, particularly in stage 1B, T2 N0 M0. These results of this study may be able to confirm the previous UFT adjuvant trial.

Meta-analysis of six randomized adjuvant trials with UFT (presented at ASCO 2004[14])

Clinical trials assessing the response of non-small cell lung cancer to postoperative adjuvant chemotherapy should use survival as the primary endpoint. Response should be evaluated by means of randomized controlled studies using surgical therapy alone as control. Single studies usually do not provide clear-cut conclusions because of limited sample size. A meta-analysis of all properly randomized clinical trials comparing long-term adjuvant chemotherapy with UFT, an oral fluorinated pyrimidine derivative, with surgery alone in patients with completely resected non-small cell lung cancer was demonstrated.

Six randomized trials have been conducted that compare surgery alone with adjuvant chemotherapy with UFT. The analysis was based on individual patient data provided by the principal investigator of each trial. In data from 2003, eligible patients were analyzed on an intention-to-treat bias. The endpoint of interest was overall survival at 5 years after surgery. Major prognostic factors were well balanced between the UFT group and surgery-alone group. Most patients had early-stage non-small cell lung cancer. The distribution of pathological T1 and T2 stages among this population was 65% and 34%, respectively.

The 5-year overall survival rate and 7-year overall survival rate were 81.8% and 76.5% and 77.2% in the control group; 7-year overall survival rates were 81.8% and 76.5% and 77.2% in the control group, and 7-year overall survival was 69.5% for the surgery-alone group. The result of meta-analysis demonstrated that adjuvant chemotherapy with UFT significantly improved the overall 5-year survival rate, with hazard ratio (HR) 0.77 (95% CI, 0.63–0.94; $P = 0.011$). Heterogeneity of effect among the six studies was not significant ($P = 0.76$).

The subset analysis of this meta-analysis indicated that UFT treatment provided a definitive survival benefit in most of the subset. This meta-analysis of the T1 subset population demonstrated that treatment with UFT provided a definitive survival benefit for patients with tumor that was 2–3 cm in diameter. Therefore, on the basis of our meta-analysis, postoperative adjuvant chemotherapy with UFT has a beneficial effect on outcome in patient with curatively resected non-small cell lung cancer more than 2 cm in size. Recently, Dr. Hotta from Okayama University has also demonstrated the benefit of UFT in the postoperative adjuvant setting based on the meta-analysis of five abstracts regarding UFT adjuvant trials (HR, 0.799; 95% CI, 0.668–0.957, $P = 0.015$).[15] These results seem to confirm the previous Hamada data.

A randomized phase III study for Bestatin (Ubenimex) as postoperative adjuvant treatment in patients with stage I squamous cell lung cancer (presented at ASCO 2001[16])

In a placebo-controlled phase III trial sponsored by the Japanese NK421 Lung Cancer Study Group, the more derived immunomodulator Bestatin (Ubenimex) was used as adjuvant therapy for patients with stage I squamous cell carcinoma following completed resection.

Confirmation of the patient eligibility and the randomization were performed within 4 weeks after each operation. The oral administration started within 1 week after their randomization. One capsule of either Bestatin or placebo was administered orally after breakfast every day for 2 years postoperatively. No additional treatment was allowed until definitive recurrence or appearance of second cancer was diagnosed.

A follow-up examination was performed every 3 months for 2 years after operation and every 6 months thereafter. The primary endpoint of the study was overall survival, and the second endpoint was disease-free survival and safe assessment. The number of patients was 202 in the Bestatin group and 198 in the placebo group. There is no significant difference in baseline characteristic of patients; 97.6% and 96.3% of the projected dose of Bestatin and placebo were administered, respectively.

The median duration follow-up for 400 patients was 77 months. Overall 5-year survival rate was significantly increased for patients receiving Bestatin compared with those receiving placebo. Disease-free survival was also significantly higher in the Bestatin group compared with placebo group, 71% versus 62%. According to multivariate analysis for survival, significant prognostic factors were performance status (PS), blood transfusion, and treatment arm.

Short summary and consideration of Japanese adjuvant trials

A couple of randomized clinical trials have demonstrated survival advantage in patients predominantly with no lymph metastasis. The effectiveness of UFT in N0 patients was confirmed. The patients with completely resected stage I non-small cell lung cancer, especially T2N0 adenocarcinoma, will benefit from adjuvant chemotherapy with UFT. UFT provides 2.5% (T2, 11.4%) benefit for absolute 5-year survival rate. HR for death in patients with stage I and T2 was 0.706 and 0.48, respectively.

Future issues for UFT adjuvant chemotherapy are to be considered as follows: (1) Do patients with stage II and/or stage III disease benefit from UFT adjuvant therapy? (2) Which regimen is better, UFT or platinum-based doublet chemotherapy in the patient with stage IB and II or III? (3) Is treatment for 1 year equivalent to treatment for 2 years? (4) What is the mechanism of UFT effectiveness in the adjuvant setting? and (5) There is need for confirmatory studies in other countries. As for Bestatin, it is necessary to do another confirmatory clinical trial.

Table 2. Potential functional mechanism of UFT and bestatin

	UFT	Bestatin
Production	5-FU derivative; tegafur and uracil	Culture filtrate of *Streptomyces olivoleticuli*
Basic concept	Antimetabolic drug	Immunomodulator
Anticancer effect (possibility)	Biochemical moduration, incidence of apotosis, inhibition of angiogenesis	Inhibition of angiogenesis Introduction of apotopsis

Table 3. The efficacy of the postoperative adjuvant chemotherapy for non-small cell lung cancer based on the pathological stage

	IALT	JBR 10	CALGB 9633	JLCRG/UFT
p-stage I	Negative	Positive (IB)	Positive (IB)	Positive
p-stage II	Negative	Positive		
p-stage IIIA	Positive			
Survival benefit[a]	4.1%	15%	12% (4-year survival)	2.5% IB 11%
HR	0.86	0.70	0.62	0.71 IB 0.48
95% CI	0.76–0.98	0.52–0.92	0.41–0.95	0.51–0.98 IB 0.29–0.81

Positive, 10% improvement for the hazard ratio
HR, hazard ratio; 95% CI, 95% confidential interval
[a]Absolute difference of the 5-year survival rate between the adjuvant group and the surgery-alone group

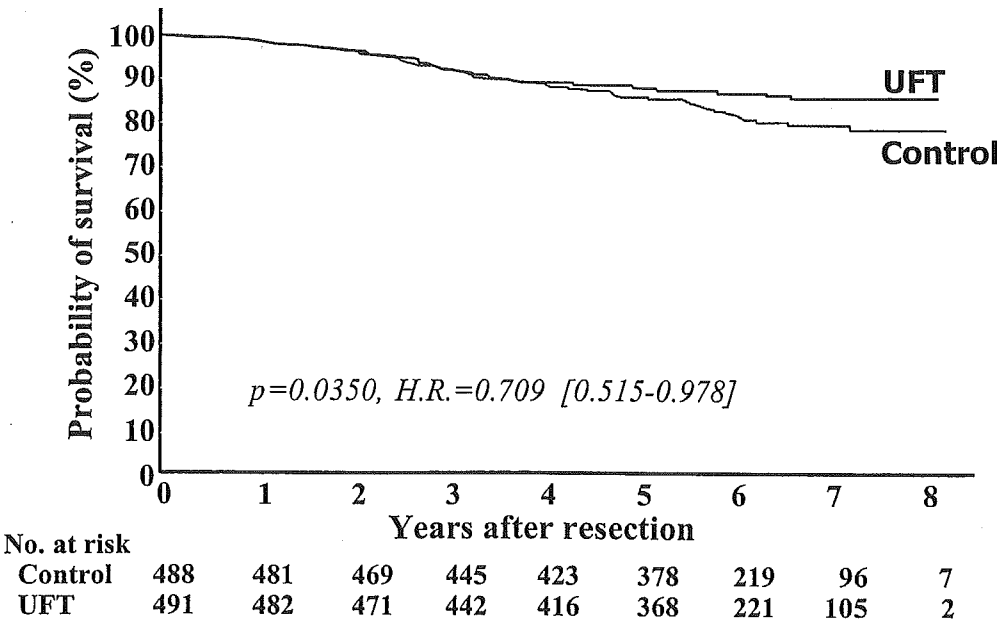

Fig. 1. Overall survival among all 979 eligible patients in the Japan Lung Cancer Research Group (JLCRG) trial. The hazard ratios indicate the risk of death in the UFT group as compared with the control group; 95% confidential intervals are shown in *brackets*. UFT, uracil-tegafur (From ref. 13 with permission)

On the basis of the comparison of mechanism between UFT and Bestatin, both drugs have been shown to inhibit angiogenesis and induce apoptosis in vivo and in vitro (Table 2). Although these data should be confirmed in future, the administration of a less cytotoxic agent and/or cytostatic drug in the adjuvant setting may improve survival for patients with early-stage non-small cell lung cancer.

Brief results of international trials

International adjuvant lung trial (IALT) (presented at ASCO 2003[17])

On the basis of a previous meta-analysis, an international adjuvant lung cancer trial was designed to evaluate the effect of cisplatin-based adjuvant chemotherapy on survival after completely resection of non-small cell lung cancer. Patients were randomly assigned either to three or four

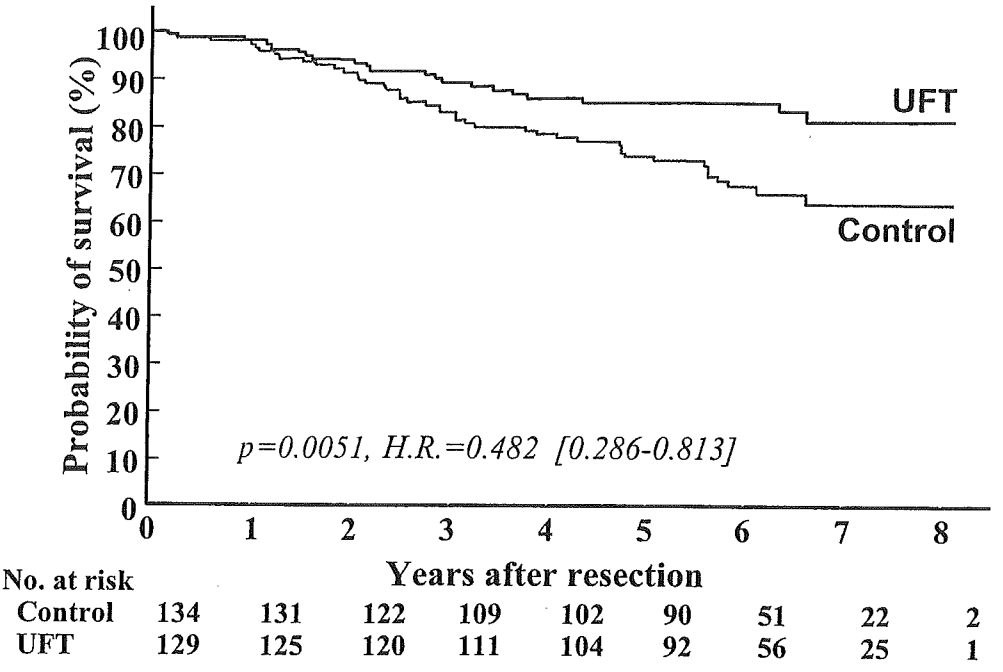

Fig. 2. Surgical outcome of T2 subset population in the JLCRG trial. UFT, uracil-tegafur (From ref. 13 with permission)

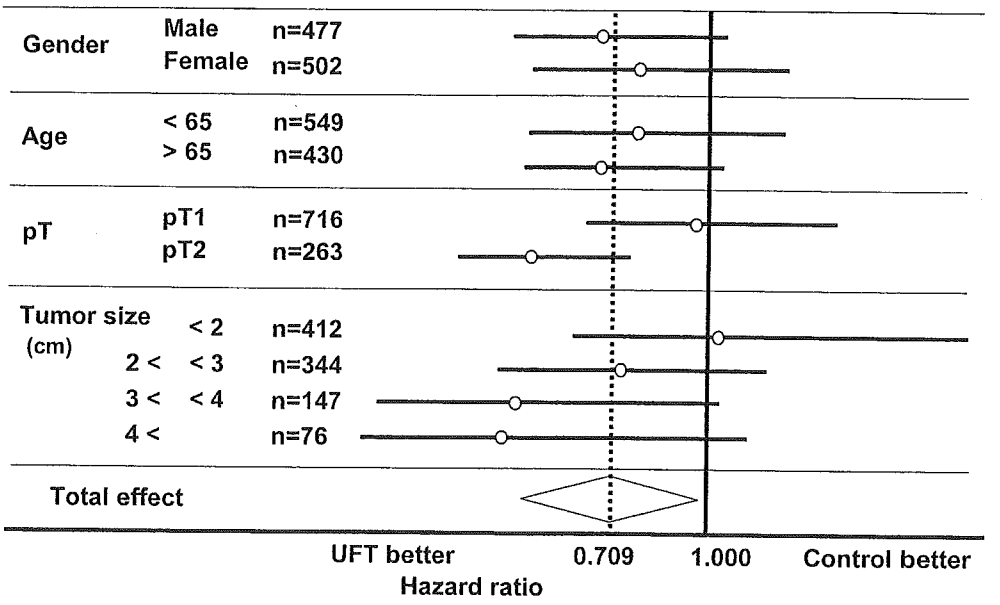

Fig. 3. Interaction in relation to treatment effect. Each *square* represents the estimated treatment effect, *horizontal lines* represent the 95% confidential intervals (CI), and the *diamond* corresponds to the 95% CI for the entire group of patients (From ref. 13 with permission)

cycles of cisplatin-based chemotherapy or to observation (without chemotherapy). Before randomization, in each center, time in the pathological stage to be included in its policy for chemotherapy and postoperative radiotherapy policy were determined. The main endpoint was overall survival.

A total of 1867 patients underwent randomization; 36.5% had pathological stage I disease, 24.2% stage II, and 39.3% stage III. The drug allocated with cisplatin was etoposide in 56.5% of patients, vindesine in 26.8%, vinblastine in 11%, and vindesine in 5.58%. Of the 932 patients assigned to chemotherapy, 73.8% received at least 240 mg cisplatin per square meter of body surface area. In total, 23% of 932 patients developed a grade 4 adverse reaction. Seven patients (0.8%) died of chemotherapy-induced toxic effects. The median duration of follow-up was 56 months. Patients assigned to chemotherapy had a significant higher survival rate than those without chemotherapy (44.5% vs. 40.4% at 5 years; HR for death, 0.86; 95% CI, 0.76–0.93; $P < 0.003$). Disease-free survival rate was also significantly different between the two group (39.4% vs. 34.3% at 5 years; HR, 0.83; 95% CI, 0.74–0.94; $P < 0.003$). Seven patients (0.8%) died of chemotherapy-related toxic events. A total of 22.6% of the patients had at least one episode of

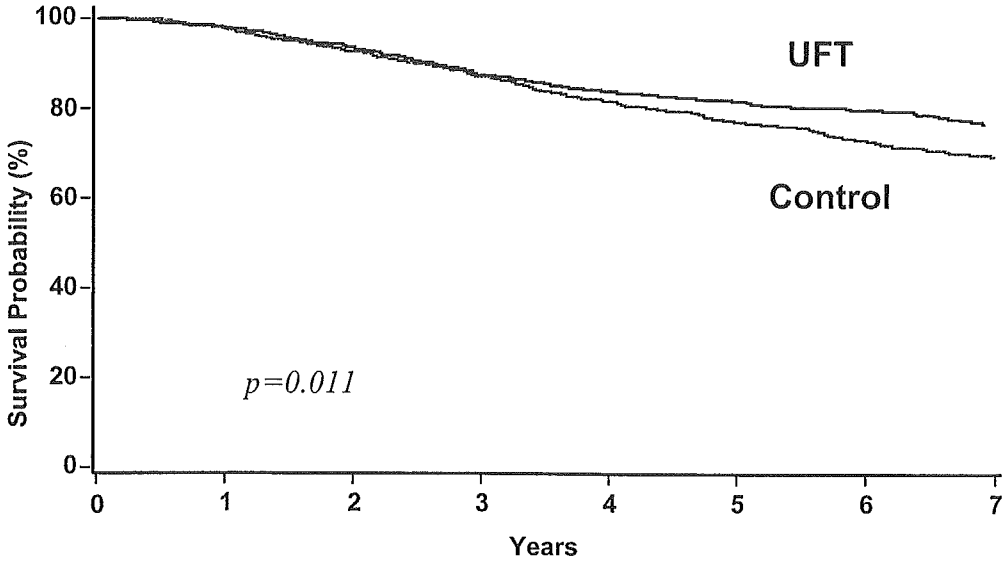

Fig. 4. Overall survival among all 2003 eligible patients in meta-analysis of six UFT trials. *P* values were calculated with stratified log-rank test (From ref. 14 with permission)

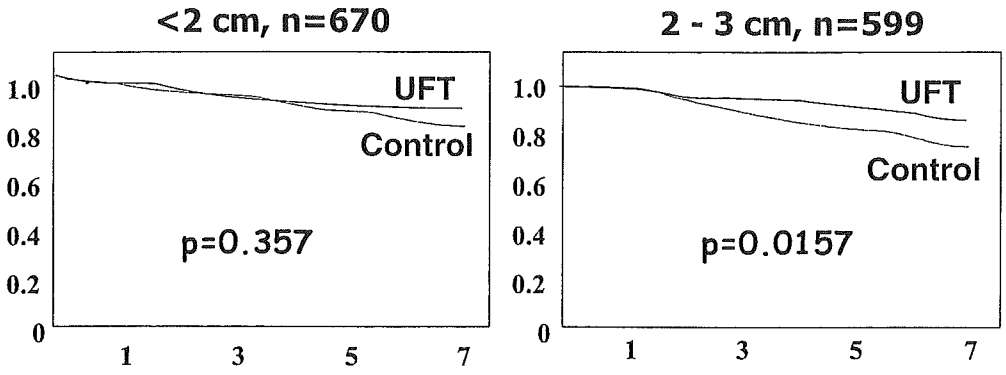

Fig. 5. Overall survival for exploratory analysis of T1 population (n = 1269) in UFT meta-analysis. *P* values were calculated with stratified log rank test (From ref. 14 with permission)

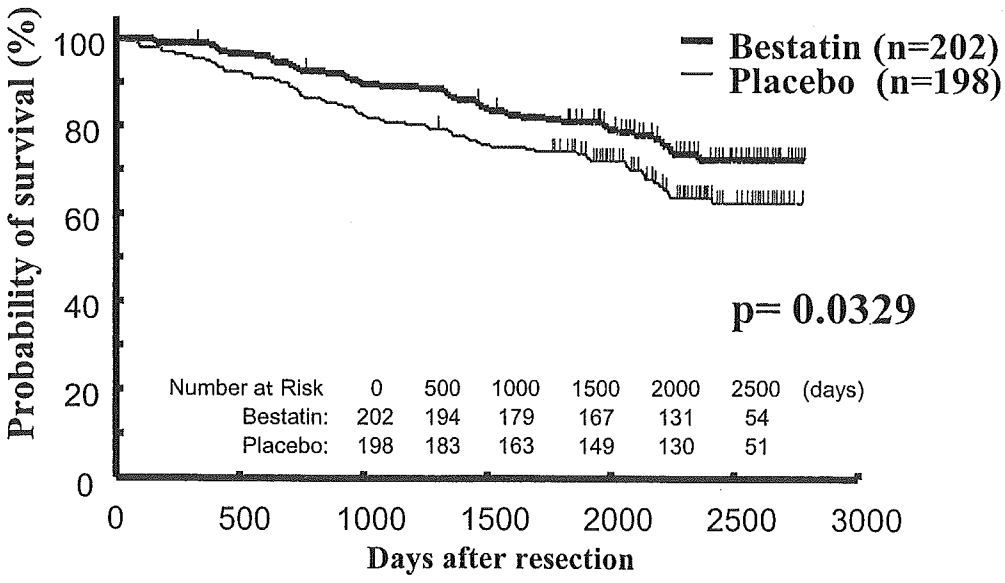

Fig. 6. Overall survival among all 400 eligible patients in Bestatin trial. *P* values were calculated with stratified log-rank test. (From ref. 16 with permission)

grade 4 toxicity, mainly neutropenia (17.5%), thrombocytopenia (2.6%), and vomiting (3.3%). These results have confirmed the meta-analysis in 1995.

NCI-Canada trial, JBR10 (presented at ASCO 2004[18])

Patients with p-stage IB and II except T3N0 were randomly assigned either to three or four cycles of cisplatin-based chemotherapy with cisplatin (50 mg/m^2, days 1, 8, every 4 weeks) or vinorelbine (25 mg/m^2, weekly to 16 weeks), or observation. A total of 344 patient underwent randomization. Stratified factors were the status of lymph node and *ras* gene. In overall survival in this study, patients with chemotherapy had a significantly higher survival rate than those with observation (69% vs. 54%, $P = 0.012$), at HR of 0.696 (95% CI, 0.524–0.923).

U.S. trial, Cancer and Leukemia Group B (CALGB) 9633 (presented in ASCO 2004[19])

Patients with p-stage IB were randomly assigned to either three or four cycles of the chemotherapy with carboplatin (AUC = 6, day 1, every 3 weeks) and paclitaxel (200 mg/m^2, day 1, every 3 weeks), or observation. A total of 482 patients underwent randomization. Stratified factors were histology, differentiation, and the status of mediastinoscopy. The median duration to follow-up was 34 months; patients assigned to chemotherapy had a significantly higher survival rate than those assigned to observation (71% vs. 59% at 4-year survival rate, $P = 0.028$). HR for this trial was 0.62 (95% CI, 0.41–0.95).

Short summary of international trials

The NCI-C and CALGB studies confirmed positive IALT results of the benefit for postoperative platinum-based chemotherapy in completely resected non-small cell lung cancer. The good results of NCI-C and CALGB trials might be due to patient selection, such as earlier-stage disease (IB and II), uniform patient population, more frequent incidence of women than ILT, and the therapeutic strategy of chemotherapy, such as a two-drug regimen with third-generation agent, better compliance, and no radiotherapy in patients without lymph node metastasis.

The summary was based on the international trial; consistent reductions in the risk of death have been observed in recent adjuvant platin-based trials and the 1995 meta-analysis. Adjuvant platinum-based chemotherapy should be recommended to completely resected non-small cell lung cancer patients with good performance status.

Consideration: future perspective

Even if completely resected stage I non-small cell lung cancer is due to recurrent disease in the majority of patients, adjuvant therapy had aimed at eradication of micrometastasis. Recent development of molecular biological techniques permits us to predict the chemotherapeutic response. In the adjuvant setting, the selection of anticancer drugs should depend on the analysis of molecular biological makers for resected materials in addition to pathological stage. In addition to cooperation with new chemotherapeutic agents, such as taxane, camptothecin, and gemcitabine, there are even newer classes of antineoplastic therapy, such as antiangiogenic inhibitor and tyrosine kinase inhibitor, that should be defined. The role of newer classes of some biological therapies with anticancer effect will be defined in coming years. The clinical benefit of platinum-based adjuvant therapy was confirmed. This paradigm is strongly recommended at stage IB and II non-small cell lung cancer. In stage IIIA, further subset analysis is necessary in the new meta-analysis, including IALT (Table 3). On the other hand, platinum-based chemotherapy has some potential of severe adverse events. Although there was no treatment-related death by carboplatin with paclitaxel in the CALGB trials, the feasibility of the platinum-based regimen in the adjuvant setting has not been confirmed yet in Japan. Careful observation after platinum-based chemotherapy is necessary.

Conclusion

Adjuvant chemotherapy for pathological stage IB to II, completely resected non-small cell lung cancer is standard care based on clinical trials. UFT showed the strongest evidence for IB in Japan. Platinum doublet chemotherapy with a third-generation anticancer agent is also recommended. Although there is no evidence of the feasibility of a platinum-based regimen in the adjuvant setting in Japan, adjuvant chemotherapy should be offered as standard care to patients after completely resected early-stage non-small cell lung cancer.

References

1. Mountain CF (1997) Revisions in international system for staging lung cancer. Chest 111:1170–1176
2. Goya T, Asamura H, Yoshimura H, et al. (2005) Prognosis of 6644 resected non-small cell lung cancers in Japan: a Japanese Lung Cancer Registry Study. Lung Cancer (in press)
3. Matthews MJ, Kanhouwa S, Pickren J, et al. (1973) Frequency of residual and metastatic tumor in patients undergoing curative surgical resection for lung cancer. Cancer Chemother Rep 4:63–68
4. Non-small Cell Lung Cancer Collaborative Group (1995) Chemotherapy in non-small cell lung cancer: a meta-analysis using updated data on individual patients from 52 randomized trials. Br Med J 311:899–909
5. Logan DM, Lochrin CA, Darling G, et al. (1997) Adjuvant radiotherapy and chemotherapy for stage II or IIIA non-small cell lung cancer after complete resection. Cancer Prevent Control 1:366–372
6. Pisters KM, Kris MG, Gralla RJ, et al. (1994) Randomized trial comparing postoperative chemotherapy with vindesine and cisplatin plus thoracic irradiation with irradiation alone in stage III (N2) non-small cell lung cancer. J Surg Oncol 56:236–241

7. Dautzenberg B, Chastang C, Arriagada R, et al. (1995) Adjuvant radiotherapy versus combined sequential chemotherapy followed by radiotherapy in the treatment of resected nonsmall cell lung carcinoma. A randomized trial of 267 patients. GETCB (Groupe d'Etude et de Traitement des Cancers Bronchiques). Cancer (Phila) 76:779–786
8. Keller SM, Adak S, Wagner H, et al. (2000) A randomized trial of postoperative adjuvant therapy in patients with completely resected stage II or IIIA non-small-cell lung cancer. N Engl J Med 343:1217–1222
9. Tada H, Tsuchiya R, Ichinose Y, et al. (2004) A randomized trial comparing adjuvant chemotherapy versus surgery alone for completely resected pN2 non-small cell lung cancer (JCOG9304). Lung Cancer 43:167–173
10. Scagliotti GV, Fossati R, Torri V, et al. (2003) Randomized study of adjuvant chemotherapy for completely resected stage I, II, or IIIA non-small-cell lung cancer. J Natl Cancer Inst 95:1453–1461
11. Wada H, Hitomi S, Teramatsu T, et al. (1996) Adjuvant chemotherapy after complete resection in non-small cell lung cancer. J Clin Oncol 14:1048–1052
12. Okimoto N, Soejima R, Teramatsu T (1996) A randomized controlled postoperative adjuvant chemotherapy trial of CDDP + VDS + UFT and UFT alone in comparison with operation only for non-small cell lung carcinomas (second study). Jpn J Lung Cancer 36:863–878
13. Kato H, Ichinose Y, Ohta M, et al. (2004) A randomized trial of adjuvant chemotherapy with uracil-tegafur for adenocarcinoma of the lung. N Engl J Med 350:1713–1731
14. Hamada C, Ohta M, Wada H, et al. (2003) Efficacy of oral UFT for adjuvant chemotherapy after complete resection of non-small cell lung cancer: meta-analysis of six randomized trials in 2003 patients. Prog Proc Eur Cancer Conf 39:S231 (abstract)
15. Hotta K, Matsuo K, Ueoka H, et al. (2004) Role of adjuvant chemotherapy in patients with resected non-small-cell lung cancer: reappraisal with a meta-analysis of randomized controlled trials. J Clin Oncol 22:3860–3867
16. Ichinose Y, Genka K, Koike T, et al. (2003) Randomized double-blind placebo-controlled trial of bestatin in patients with resected stage I squamous-cell lung carcinoma. J Natl Cancer Inst 95:605–611
17. Arriagada R, Bergman B, Dunant A, et al. (2004) Cisplatin-based adjuvant chemotherapy in patients with completely resected non-small-cell lung cancer. N Engl J Med 350:351–362
18. Winton TL, Livingstan R, Johnson D, et al. (2004) A prospective randomized trial of adjuvant vinorelbine (VNR) and cisplatin (CIS) in completely resected stage Ib and II non-small cell lung cancer (NSCLC) Intergroup JBR 10. J Clin Oncol 22:621
19. Strauss GM, Hernden J, Maddaus MA, et al. (2004) Randomized clinical trial of adjuvant chemotherapy with paclitaxel and carboplatin following resection in stage Ib non-small cell lung cancer (NSCLC): report of Cancer and Leukemia Group B (CALGB) protocol 9633. J Clin Oncol 22:621

Expression pattern of the scaffold protein IQGAP1 in lung cancer

HARUHIKO NAKAMURA[1], KOJI FUJITA[2], HIRAKU NAKAGAWA[4], FUKUKO KISHI[4], ATSUSHI TAKEUCHI[4], IDIRIS AUTE[3] and HARUBUMI KATO[3]

[1]Department of Respiratory Surgery, Atami Hospital, International University of Health and Welfare; Departments of [2]Pathology and [3]Surgery, Tokyo Medical University; [4]ProteinExpress Co., Ltd., Japan

Received August 12, 2004; Accepted November 17, 2004

Abstract. IQGAP1 is a scaffold protein whose function relates to signal transduction, cell adhesion, local invasion, and distant metastasis of cancer cells. We examined the expression patterns of this protein and clinicopathologic features of lung cancer, and the antibody against IQGAP1 was used for immunohistochemical analysis. Of the 70 surgical specimens examined, there were 40 adenocarcinomas, 19 squamous cell carcinomas, 5 large cell carcinomas, 3 small cell carcinomas, 2 carcinoid tumors, and 1 mucoepidermoid carcinoma. The localization of IQGAP1 was classified into three types: 1) cytoplasmic, 2) membranous, and 3) reduced expression. In adenocarcinoma, the 3 types were observed equally, and differentiation grade was related to the expression pattern. The cytoplasmic type was common in well-differentiated adenocarcinomas, and membranous or reduced expression was frequently seen in moderately- or poorly-differentiated adenocarcinomas. In squamous cell carcinoma, the membranous type was most common. Although the staining pattern of IQGAP1 did not correlate with the positivity of regional lymph nodes, survival in those patients with a cytoplasmic type was significantly better than others with adenocarcinoma (p=0.0144). Expression typing of IQGAP1 in lung cancer was associated with histologic type and can be used to predict survival in patients with adenocarcinoma of the lung.

Introduction

In cancer cells, abnormal protein expression affects signal transduction, cell adhesion, local invasion, and distant metastasis. IQGAP proteins are multidomain molecules that contain several protein-interacting motifs, and IQGAP1 is a component of signaling networks that are integral to maintaining cytoskeletal architecture and cell adhesion (1). These functions include modulating the actin cytoskeleton (2), mediating signaling by the Rho family GTPases (3) and calmodulin (4), and regulating the E-cadherin and ß-catenin function (5,6).

Recent microarray analysis has revealed that highly-metastatic mouse melanoma cells have gene expression of IQGAP1 increased by >2.5-fold (7). In human clinical cases, IQGAP1 was overexpressed in colon cancer compared with normal tissue, and IQGAP1 tended to be expressed more at the invasive front (8). These reports imply that IQGAP1 may play an important role in tumor development and malignant behavior.

We performed an immunohistochemical analysis using a newly-developed specific antibody against IQGAP1 to elucidate the relationship between expression patterns of IQGAP1 and clinicopathologic features of patients with lung cancer.

Patients and methods

Patients. The patients included 45 men and 25 women with an average age of 63 years. Lobectomy and mediastinal lymph node dissection were performed in all cases, and no pre-surgical chemotherapy or radiotherapy was administered. The diagnosis of lung cancer was established by histologic examination of the surgical specimens (9), and TNM staging was performed using the latest criteria (10) with results showing pathologic stage IA in 19, IB in 15, IIA in 2, IIB in 12, IIIA in 13, IIIB in 5, and IV in 4 cases. Informed consent for immunohistochemical analysis of the primary lung cancer was obtained from all patients, and the median follow-up period of the censored cases was 60 months.

Tissue samples. The tissue samples were fixed in buffered formaldehyde and stored as paraffin-embedded blocks until use. Distribution of the IQGAP1 antigen in normal human tissues was examined using NormalGrid™ Multi-Tissue control slides (Biomeda Corp., Foster City, CA).

Generation of specific antibody against IQGAP1. We selected a cDNA clone (KIAA0051) coding IQGAP1 from the Kazusa cDNA library to generate a specific antibody for immunohistochemistry. We screened the HUGE database, which contains human novel large cDNAs identified in the Kazusa cDNA sequencing project (11) and is available at

Correspondence to: Dr Haruhiko Nakamura, Department of Respiratory Surgery, Atami Hospital, International University of Health and Welfare, 13-1 Higashikaigan-cho, Atami-city, 413-0012 Shizuoka, Japan
E-mail: h.nakamura@iuhw.ac.jp

Key words: adenocarcinoma, carcinogenesis, cytoskeleton, immunohistochemistry, survival

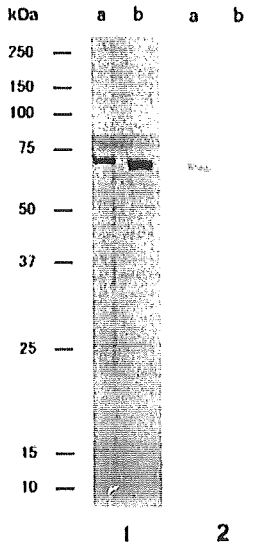

Figure 1. Western blot analysis of the reactivity of affinity-purified anti-IQGAP1 antibody (KD0019). Lane 1 indicates the results of SDS-PAGE stained by Coomassie Brilliant Blue. (a) Purified maltose-binding protein-fusion protein carrying the antigenic region of IQGAP1, and (b) control protein. Lane 2 indicates the results of Western blot analysis reacted with affinity-purified anti-IQGAP1 antibody, KD0019. (a) Purified maltose-binding protein-fusion protein carrying the antigen region of IQGAP1, and (b) control protein.

http://www.kazusa.or.jp/huge. Using KIAA0051 as a template, a DNA fragment coding 200 amino acids (E201-N400) was amplified by polymerase chain reaction (5' primer, CGC GGATCCGAAGAAATCAACAACATGAAGACTG; and 3' primer, CCCAAGCTTCTAGTTTGCAGCATCCACTCC AGACTGC), fused to the plasmid pDEST15 and propagated in *Escherichia coli*. The protein was purified and used as an immunogen. A rabbit was immunized with the purified IQGAP1, and antiserum was purified with N-hydroxy-succinimide (NHS)-activated Sepharose 4 Fast Flow (Amersham Biosciences, Piscataway, NJ) bound with the same antigen protein. The purified rabbit-specific antibody against IQGAP1 was named KD0019 and used for immunohistochemistry.

Western blot analysis confirms the reactivity of affinity-purified anti-IQGAP1 antibody, KD0019. To verify the specificity of KD0019, 1.2 μg of purified maltose-binding fusion protein carrying the antigen region of IQGAP1 or a control sequence was separated by sodium dodecyl sulfate-polyacrylamide gel electrophoresis (SDS-PAGE), followed by transfer onto a polyvinylidene fluoride (PVDF) membrane. The blotted membrane was reacted with KD0019 or affinity-purified control antibody, followed by alkaline phosphatase-conjugated anti-rabbit IgG antibody (7500-fold dilution) (Promega, Madison, WI). The immunoreactive proteins were visualized with the bromo-chloro-iodoryl phosphate (BCIP)/nitro-blue tetrazolium (NBT) color development substrate (Promega).

Immunohistochemistry. The streptavidin-biotin peroxidase complex (SABC) technique was used for immunohistochemical staining. Sections (4 μm thick) were cut, kept in xylene, rehydrated and washed with water, then treated with 0.3% hydrogen peroxide in methanol for 10 min to inhibit endogenous peroxidase and autoclaved in a citrate buffer solution (10 mM sodium citrate, pH 6.0) at 100°C for 20 min to retrieve antigenicity. After blocking non-specific binding with 5% normal rabbit serum, sections were incubated with primary antibody, KD0019 (500 ng/ml) at 4°C overnight. Slides were then washed and incubated with a second antibody, biotinylated anti-rabbit IgG (LSAB kit) (Dako, Copenhagen, Denmark) for 15 min at room temperature. Finally, the slides were washed and incubated with SABC Elite reagent (Dako) for 15 min at room temperature. Specific staining was developed with diaminobenzidine tetrahydrochloride supplemented with 0.03% hydrogen peroxide and counterstained with hematoxylin, and lung cancers were classified into three types according to the staining pattern of IQGAP1: 1) cytoplasmic (C-type), 2) membranous (M-type), and 3) reduced expression (R-type).

Table I. The staining pattern of IQGAP1 according to the histologic type of lung cancer.

Staining pattern	Histologic type					Total
	Ad	Sq	La	Sm	Mis	
C-type	15	4	1	3	2	25
M-type	14	13	1	0	0	28
R-type	11	2	3	0	1	17
Total	40	19	5	3	3	70

Ad, adenocarcinoma; Sq, squamous cell carcinoma; La, large cell carcinoma; Sm. small cell carcinoma; Mis, miscellaneous tumors; C-type, cytoplasmic type; M-type, membranous type; R-type, reduced expression type.

Statistical analysis. Differences between groups were evaluated using the χ^2 test, the survival rate was calculated by the Kaplan-Meier method, and survival differences were compared using the log-rank test as a univariate analysis. $p<0.05$ was considered significant.

Results

Specificity of anti-IQGAP1 antibody. Affinity-purified anti-IQGAP1 antibody, KD0019, strongly reacted with the maltose-binding IQGAP1 fusion protein, but not the control molecule (Fig. 1).

Localization of IQGAP1 in normal human tissues. In normal lung tissues, strong staining was observed in alveolar macrophages, bronchial epithelium, and bronchial glands. In bronchial glands, localization of IQGAP1 was limited to the cytoplasm and cell boundaries of serous glands; no mucous glands were stained (Fig. 2A). Skin, epithelium of the external glands of the prostate, Kupffer cells, and distal urinary tubules in the kidney all showed relatively strong staining (Fig. 2B-E). Skin showed the strongest positive reaction in both the cell membrane and cytoplasm. Only weak staining was observed in the spleen, uterus, placenta,

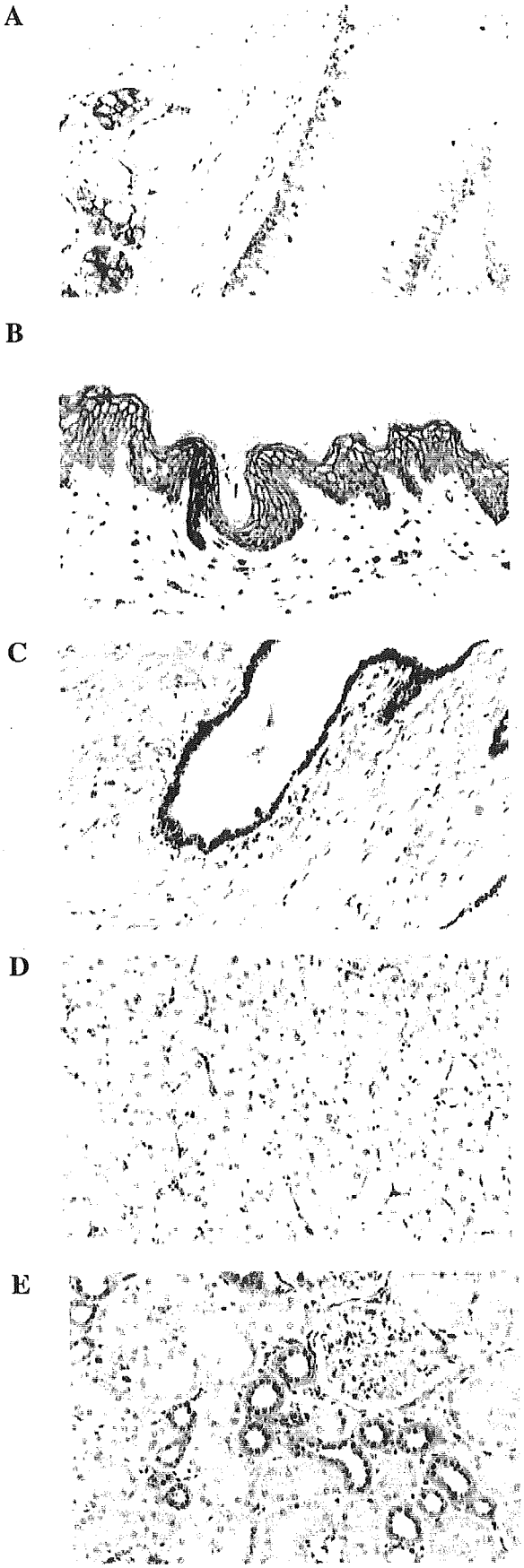

Figure 2. The distribution of IQGAP1 in normal lung. IQGAP1 strongly stained (A) bronchial epithelium and serous glands in normal lung, (B) normal skin, (C) external glands of the prostate, (D) Kupffer cells, and (E) distal urinary tubules in the kidney.

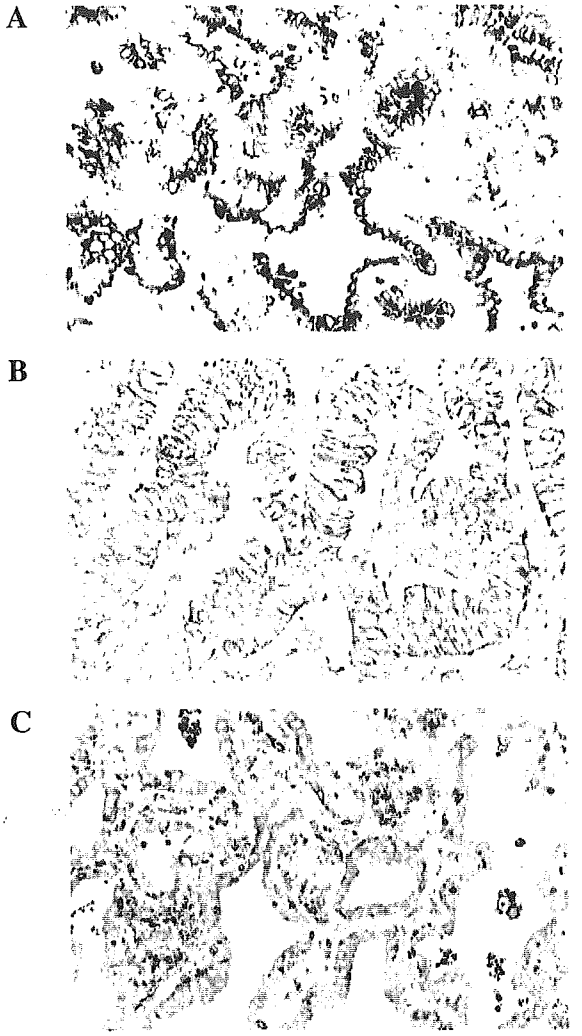

Figure 3. Representative staining patterns of IQGAP1 in lung cancer. Adenocarcinomas showing (A) cytoplasmic, (B) membranous, and (C) reduced expression type.

tonsil, testis, ovary, pancreas, breast, heart, stomach, small and large intestine, brain, pituitary gland, and adrenal gland.

Localization of IQGAP1 in lung cancer

Expression pattern according to histologic type. Of the 70 surgical specimens examined, there were 40 adenocarcinomas, 19 squamous cell carcinomas, 5 large cell carcinomas, 3 small cell carcinomas, 2 carcinoid tumors, and 1 mucoepidermoid carcinoma. A representative staining pattern is shown in Fig. 3A-C. In squamous cell carcinoma, M-type was frequently seen (68.4%, 13/19); in adenocarcinomas, the 3 types were equally observed (Table I). All 3 small cell lung cancers and 2 carcinoids showed weak cytoplasmic staining.

Expression pattern and grade of differentiation of lung cancer. In adenocarcinoma, differentiation grade was related to the expression pattern (Table II). C-type was common in well-differentiated adenocarcinoma, and M- and R- types were frequently seen in moderately- and poorly-differentiated adenocarcinoma (p=0.0004). In squamous cell carcinoma, a difference in staining pattern according to differentiation grade was not observed (p=0.3960).

Table II. The staining pattern of IQGAP1 according to the differentiation grade of lung cancer.

Staining pattern	Ad			Sq			Total
	WD	MD	PD	WD	MD	PD	
C-type	10	5	0	1	1	2	19
M-type	2	9	3	3	9	1	27
R-type	1	6	4	0	0	2	13
Total	13	20	7	4	10	5	59

Ad, adenocarcinoma; Sq, squamous cell carcinoma; La, large cell carcinoma; Sm. small cell carcinoma; Mis, miscellaneous tumors; C-type, cytoplasmic type; M-type, membranous type; R-type, reduced expression type.

Table III. The staining pattern of IQGAP1 according to nodal status.

Staining pattern	Ad		Sq		Total
	N(-)	N(+)	N(-)	N(+)	
C-type	12	3	2	2	19
M-type	7	7	6	7	27
R-type	4	7	0	2	13
Total	23	16	8	11	59

N(-), node negative; N(+), node positive; Ad, adenocarcinoma; Sq, squamous cell carcinoma; C-type, cytoplasmic type; M-type, membranous type; R-type, reduced expression type.

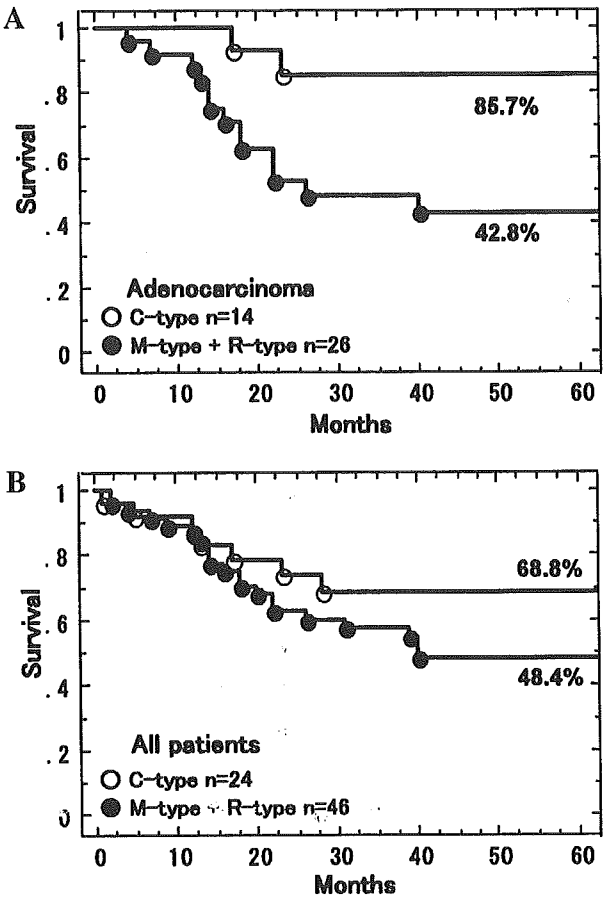

Figure 4. Kaplan-Meier survival curves after resection of lung cancer. (A) Staining pattern of IQGAP1 was significantly related to survival in patients with adenocarcinoma (p=0.0144). (B) Staining pattern of IQGAP1 was not related to survival when all patients were analyzed together (p=0.2363).

Expression pattern and nodal status. Staining patterns of IQGAP1 did not correlate with positivity of the regional lymph nodes (Table III).

Expression pattern and survival of patients with lung cancer. In adenocarcinoma, a survival difference was observed between the C group and the M and R groups (p=0.0144; Fig. 4A). This difference was not observed in all cases of lung cancer or other histologic types (p=0.2363; Fig. 4B).

Discussion

IQGAP1 is a scaffold protein that plays an important role in molding the cytoskeleton, signal transduction, and intercellular adhesion, and co-localizes with actin filaments in the cell cortex. It binds *in vitro* to F-actin and several signaling proteins, including calmodulin, Cdc42, Rac1, and ß-catenin (12,13). F-actin binding activity of IQGAP1 is regulated by its reversible association with these signaling molecules, but the mechanism is unclear (14).

Previously, localization of IQGAP1 in malignant tumors had only been examined in adenocarcinomas, and gastric, colon, and endometrial cancer. In gastric cancer, IQGAP1 was frequently observed diffusely in the cytoplasm in intestinal-type, well-differentiated tumors, but it was expressed at the cell membrane in diffuse-type, poorly-differentiated tumors (15). In that report, E-cadherin was localized to the cell membrane of the well-differentiated type and in the cytoplasm of poorly-differentiated tumors; thus, subcellular localization of IQGAP1 was inversely correlated with E-cadherin localization. Movement of IQGAP1 from the cytoplasm to the cell membrane could be correlated with E-cadherin dysfunction and dedifferentiation in gastric carcinogenesis. In colorectal cancer, IQGAP1 seemed to be expressed more at the invasion front of the tumor, and this expression pattern was most apparent in advanced disease (8). In endometrial cancer, α-catenin and IQGAP1 were absent from cell adhesive sites in well-differentiated adenocarcinomas (16). All of these results suggest that the differential grade of adenocarcinomas is associated with abnormal intracellular localization of IQGAP1.

Lung cancer has four major histologic types: 1) adenocarcinoma, 2) squamous cell carcinoma, 3) small cell carcinoma, and 4) large cell carcinoma, unique from other cancers. Thus, we were interested in IQGAP1 expression according to the histologic type of lung cancer. In normal tissues, we demonstrated that stratified squamous epithelium showed strong staining in both cytoplasm and cell boundaries in skin. Therefore, it is not surprising that squamous cell